IBRO Neuroscience Reports 15 (2023) 364–375

Contents lists available at ScienceDirect

IBRO Neuroscience Reports

journal homepage: www.sciencedirect.com/journal/IBRO-Neuroscience-Reports

Research paper

Time-on-task effects on human pupillary and saccadic metrics after theta burst transcranial magnetic stimulation over the frontal eye field

Chin-An Wang [a,b,c,*], Neil G. Muggleton [d,e], Yi-Hsuan Chang [d], Cesar Barquero [c,d,f], Ying-Chun Kuo [a,b,c]

[a] Department of Anesthesiology, School of Medicine, College of Medicine, Taipei Medical University, Taipei City, Taiwan
[b] Department of Anesthesiology, Shuang Ho Hospital, Taipei Medical University, New Taipei City, Taiwan
[c] Eye-Tracking Laboratory, Shuang Ho Hospital, Taipei Medical University, New Taipei City, Taiwan
[d] Institute of Cognitive Neuroscience, College of Health Science and Technology, National Central University, Taoyuan City, Taiwan
[e] Cognitive Intelligence and Precision Healthcare Center, National Central University, Taoyuan City, Taiwan
[f] Department of Physical Activity and Sport Science, Universidad Peruana de Ciencias Aplicadas, Lima, Peru

ARTICLE INFO

Keywords:
CTBS
Pupillary light reflex
Pupillometric
Superior colliculus
Attention

ABSTRACT

Pupil size undergoes constant changes primarily influenced by ambient luminance. These changes are referred to as the pupillary light reflex (PLR), where the pupil transiently constricts in response to light. PLR kinematics provides valuable insights into autonomic nervous system function and have significant clinical applications. Recent research indicates that attention plays a role in modulating the PLR, and the circuit involving the frontal eye field (FEF) and superior colliculus is causally involved in controlling this pupillary modulation. However, there is limited research exploring the role of the human FEF in these pupillary responses, and its impact on PLR metrics remains unexplored. Additionally, although the protocol of continuous theta-burst stimulation (cTBS) is well-established, the period of disruption after cTBS is yet to be examined in pupillary responses. Our study aimed to investigate the effects of FEF cTBS on pupillary and saccadic metrics in relation to time spent performing a task (referred to as time-on-task). We presented a bright stimulus to induce the PLR in visual- and memory-delay saccade tasks following cTBS over the right FEF or vertex. FEF cTBS, compared to vertex cTBS, resulted in decreased baseline pupil size, peak constriction velocities, and amplitude. Furthermore, the time-on-task effects on baseline pupil size, peak amplitude, and peak time differed between the two stimulation conditions. In contrast, the time-on-task effects on saccadic metrics were less pronounced between the two conditions. In summary, our study provides the first evidence that FEF cTBS affects human PLR metrics and that these effects are modulated by time-on-task.

Introduction

The pupil transiently constricts in response to a global increase in luminance, known as the pupillary light reflex (PLR) (Loewenfeld, 1999). This reflex serves to regulate the amount of light reaching the retina, optimizing the balance between visual sensitivity and acuity (Woodhouse, 1975; Laughlin, 1992). The PLR involves measuring response dynamics, including response onset latency, amplitude, peak velocity, the pupil main sequence slope (peak velocity/amplitude), and time to reach peak amplitude (together referred to as pupillary metrics). Extensive research has shown that pupillary metrics provide valuable insights into the control of pupil size and are crucial for clinical investigations (Steinhauer and Hakerem, 1992; Kardon, 1995; Loewenfeld, 1999; Barbur, 2004; Yu et al., 2007; Hall and Chilcott, 2018). Despite the PLR being a reflex, evidence suggests that it is modulated by various high-level cognitive processes such as attention (Binda and Gamlin, 2017). Studies have demonstrated that a bright stimulus elicits a larger PLR when it is spatially aligned with attention compared to when it is not (e.g., Binda and Murray, 2015; Mathôt and Van der Stigchel, 2015).

A network of brain areas is involved in the control of gaze and attention shifts (Thompson and Bichot, 2005; Krauzlis et al., 2013), including the superior colliculus (SC) in the midbrain and the frontal eye fields (FEF) in the prefrontal cortex. The SC anatomically and

* Corresponding author at: Department of Anesthesiology, School of Medicine, College of Medicine, Taipei Medical University, Taipei, Taiwan.
E-mail address: josh.wang@tmu.edu.tw (C.-A. Wang).

https://doi.org/10.1016/j.ibneur.2023.11.001
Received 25 July 2023; Received in revised form 1 October 2023; Accepted 1 November 2023
Available online 8 November 2023

functionally connects with the FEF (Komatsu and Suzuki, 1985; Segraves and Goldberg, 1987; Stanton et al., 1988; Schlag-Rey et al., 1992; Everling and Munoz, 2000; Sommer and Wurtz, 2000), and projects directly to the premotor circuit in the brainstem to initiate saccade generation (Moschovakis et al., 1988; Rodgers et al., 2006). The SC and FEF are not only causally involved in gaze and attention shifts (Thompson and Bichot, 2005; Gandhi and Katnani, 2011; Johnston and Everling, 2011; White et al., 2011; Krauzlis et al., 2013), but also play a central role in the control of pupil size (Wang and Munoz, 2015,2023). Microsimulation of the SC or FEF evokes transient pupillary dilation in behaving monkeys (Wang et al., 2012; Joshi et al., 2016; Lehmann and Corneil, 2016). Trial-by-trial correlations between pupillary and saccadic responses evoked by SC microstimulation have also been noted (Wang and Munoz, 2021,2023). Importantly, PLR responses induced by a bright stimulus were larger when the stimulus was presented at a location spatially aligned with the stimulated FEF region (Ebitz and Moore, 2017). These results together provide clear evidence for the involvement of the FEF in mediating pupillary luminance responses modulated by high-level cognition in monkeys. However, investigations into the causal role of the FEF in human pupillary responses are very limited.

Transcranial magnetic stimulation (TMS) is a powerful tool for noninvasively investigating the causal role of different brain areas in specific functions of interest (Sack, 2006). Continuous theta-burst transcranial magnetic stimulation (cTBS) has been developed to disrupt a target region for up to 1 h following this rapid stimulation protocol (Huang et al., 2005). More specifically, this seminal study found that cTBS over the human motor cortex produces disruption that outlasts the period of stimulation by more than 60 min. However, research examining the time-on-task effects of cTBS on other response measurements is limited. Previous studies using cTBS over the right FEF have demonstrated some disruptions in human pupillary responses (Hsu et al., 2021, 2022). Nevertheless, the time-on-task effects of FEF cTBS on pupillary responses have yet to be examined. Furthermore, the effects of FEF cTBS on pupillary metrics remain unexplored.

To investigate the time-on-task effects of FEF cTBS on human pupillary and saccadic metrics, we administered cTBS over the right FEF and the vertex, utilizing magnetic resonance imaging-guided TMS. Moreover, a bright stimulus was presented to induce PLR responses during the delay period in the visual- and memory-delay saccade tasks. We hypothesized that if there were time-on-task effects of FEF cTBS on pupillary and saccadic metrics, then an interaction between the trial sequence and the stimulation condition should be observed, resulting in differences in the time-on-task modulation between the two stimulation conditions.

Methods and materials

Experimental setup

All experimental procedures were reviewed and approved by the Institutional Review Board of the Taipei Medical University, Taiwan, and were in accordance with the Declaration of Helsinki (World Medical Association, 2001). Twenty-eight healthy participants (8 males, mean age: 28.1, SD: 3.8 years) from Taipei Medical University were recruited. Participants had normal or corrected-to-normal vision and were naïve regarding the purpose of the experiment. Participants provided informed consent and were compensated financially for their participation. Sample sizes were chosen based on our previous studies with comparable pupil size and saccades measurements and trial numbers per participant (Wang et al., 2018; Hsu et al., 2020, 2021; Cherng et al., 2021). We reanalyzed a dataset from a previous publication (Hsu et al., 2022), with a specific focus on examining the time-on-task effects of FEF cTBS on pupillary and saccadic metrics. Some aspects of analyses related to pupillary and saccadic responses have been published previously (Chen et al., 2022; Hsu et al., 2022).

Recording and apparatus

Participants were seated in a dark room. As described previously (Hsu et al., 2022), eye position and pupil size were measured with a video-based eye tracker (Eyelink-1000 plus binocular-arm, SR Research, Osgoode, ON, Canada) at a rate of 500 Hz with binocular recording (data from the left pupil was used for analysis), and stimulus presentation and data acquisition were controlled by the Eyelink Experiment Builder. Stimuli were presented on an LCD monitor at a screen resolution of 1920 × 1080 pixels with a 60 Hz refresh rate, subtending a viewing angle of 58° x 32°, with the distance from the eyes to the monitor set at 60 cm.

Theta-burst stimulation

As described in detail previously (Hsu et al., 2022), we carefully followed the cTBS protocol of Huang et al., (2005) to disrupt right FEF activity. We stimulated the right FEF because brain networks within the right hemisphere are more involved in supporting attention systems (Heilman and Van Den Abell, 1980; Bartolomeo and Seidel Malkinson, 2019). We used MRI-guided TMS neuronavigation with Talairach coordinates to optimize the accuracy of the location of stimulation in individual subjects (Sack et al., 2009). Briefly, T1-weighted images of MRI were acquired for each subject using 3 T General Electric Discovery MR750 scanner with an 8-channel head coil and the Talairach coordinates [33 5.1 65] were used for the location of the right FEF (Muggleton et al., 2003). Brainsight 2 (Rogue Research Inc., Canada) was used to localize the FEF for each participant, and the vertex was manually measured and used as a control stimulation site. The cTBS pulses were administered with a Magpro X100 (MagVenture, Denmark) and a 70 mm figure-of-eight-shaped coil (MC-B70, MagVenture). Each cTBS session involved delivery of a 40 s train of uninterrupted biphasic theta-burst pulses. This consisted of trains of 3 pulses, with pulses delivered at 50 Hz and trains initiated every 200 ms, giving a total of 600 pulses over 40 s and using stimulation intensity of 80 % of active motor threshold (AMT), which was applied over each brain region. These parameters followed the recommendations of the TMS safety guidelines (Rossi et al., 2009). To determine the AMT to allow selection of the 80 % stimulation intensity, motor evoked potentials were elicited by placing the coil oriented 45 degrees to the coronal plane and measured the response from the right first dorsal interosseous hand muscle using electromyography (MP160, Biopac). The AMT was defined as the lowest stimulator output in percentage that elicited 5 out of 10 twitches of more than 200 μV peak-to-peak amplitude in the contralateral hand, while the participant maintained 20 % of a finger-thumb contraction (Huang et al., 2005). The mean AMT was 41.03 % ± 6.15 (mean ± standard deviation) of maximum stimulator output. The participants came in twice for the same experiment with FEF or vertex stimulation, with a one week interval between the two experiments. The sequence of stimulation sites was counterbalanced across participants.

Visual- and memory-delay saccade task (Fig. 1)

We used the visual-delay and memory-delay saccade tasks to compare both visually-guided and memory-guided saccades (Sommer and Wurtz, 2000, 2001), with a bright stimulus presented during the delay period to induce PLR responses, to investigate pupillary as well as saccadic metrics between the FEF and vertex stimulation conditions. The visual-delay and memory-delay patch paradigm (Wang et al., 2018) was modified to appropriately implement cTBS in the tasks. Participants were seated in a dark room for the two tasks of the experiment (visual- and memory-delay) which were intermixed within a block of 335 trials lasting approximately 45 min. In the visual-delay task, each trial began with the appearance of a central fixation point (FP) (0.5° diameter; ~10 cd/m^2) on a black background (~0.01 cd/m^2). After a variable delay (800–900 ms), a peripheral colored target (0.5° diameter; ~45 cd/m^2;

referred to as the target stimulus) appeared to the right or left (radial angle: 0 or 180°) at an eccentricity of 7, 8, or 9° of visual angle from the central FP. After a variable delay (400 – 700 ms), a bright circular patch was displayed briefly for 50 ms (6° in diameter, ~50 cd/m^2, referred to as the patch stimulus). After another variable delay (1200 – 1350 ms), the FP was removed, and participants were required to generate a saccade toward the target. Two types of patch stimulus conditions were used (each condition had ~40% of trials): in the consistent condition, the patch stimulus location was spatially aligned with the target location. In the inconsistent condition, the patch was presented in the mirror location of the target stimulus. In catch trials (~10% of trials), no patch stimulus was presented, such that after a variable delay (400 – 700 ms) following the target onset, the FP was removed and participants were required to generate a saccade toward the target (these catch trials were excluded from analysis). In the memory-delay task, the configuration was identical to visual-delay configuration except that the target was only presented for 100 ms. Task condition (visual-delay or memory-delay), target location (left and right) and patch location (left and right) were randomly interleaved.

Data analysis

Saccade reaction time (SRT) was defined as the time from fixation disappearance to the first saccade away from fixation (eye velocity exceeded 30°/s) with an amplitude greater than 3°. Trials were scored as correct if the first saccade after target stimulus appearance was in the correct direction (toward the target). Failure to initiate a saccade within 1200 ms after the disappearance of FP or with SRTs < 70 ms were considered as outliers and were excluded from analysis (< 1% of trials). To maintain accurate measurement of pupil size around the patch presentation period, trials with an eye position deviation of more than 2° from the central FP or with detected saccades (> 2° amplitude) during the period from 500 ms before to 1200 ms after patch onset were excluded from analysis. When blinks were detected, following the

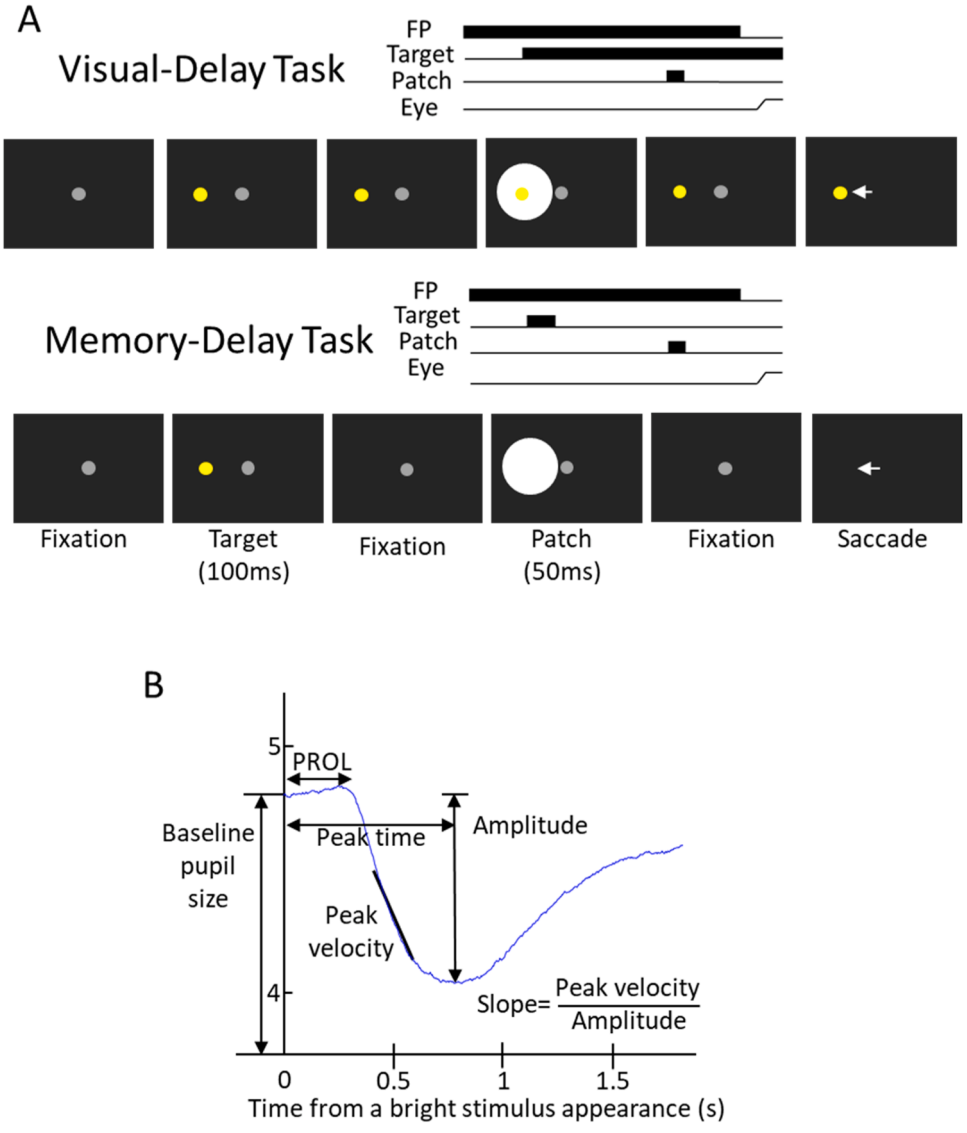

Fig. 1. (A) Experimental paradigm. Each trial started with a central fixation point on a black background. After a delay, there was presentation of a target stimulus, and after a random delay the central fixation point disappeared and participants were required to move their eyes to the target. During the delay period, a bright circular patch stimulus was presented briefly (50 ms), with the patch being spatially aligned with the target location or the opposite location of the target in the consistent and inconsistent condition, respectively. The memory-delay task was similar to the visual-delay task except the target stimulus was only presented briefly (100 ms). Note that the figure only shows left-target conditions for illustration of the paradigm. (B) Measurements of pupillary metrics**.** PROL: pupil response onset latency. Peak Velocity: peak pupil constriction velocity. Amplitude: peak pupil constriction size. Slope: pupil main sequence slope, peak velocity / amplitude. PeakTime: time to peak constriction.

literature, pre- and post-blink pupil values were used to perform a linear interpolation to replace pupil values during the blink period (Karatekin et al., 2010; Nassar et al., 2012; Mathôt et al., 2018; Cherng et al., 2020). Trials with different target and patch location conditions were collapsed to focus on the time-on-task effects between the FEF and vertex stimulation conditions. Note that outlier values in saccade reaction times, and saccadic and pupillary peak velocities beyond 1.5 times the interquartile range (the difference between upper and lower quartiles) below the lower quartile or above the upper quartile were excluded from analysis. To ensure there were enough valid trials across different points in time during the task, we first sorted trials into 8 time bins according to time-on-task (i.e. trial sequence) in each condition (e.g., Fig. 2). One participant with less than 5 trials in the first time bin was thus excluded. The remaining participants had 13.7 ± 2.4 (mean ± standard error) in each time bin for each condition.

Pupillary metrics were analyzed (Steinhauer and Hakerem, 1992; Kardon, 1995; Loewenfeld, 1999; Barbur, 2004; Yu et al., 2007; Hall and Chilcott, 2018), and five pupillary indices were reported (Fig. 1B). We first analyzed tonic pupil size at the baseline epoch (absolute baseline pupil diameter) for each trial, a baseline value was determined by averaging pupil size from 100 ms before to the appearance of the patch bright stimulus. Following the procedures of baseline-correction used previously (Mathôt et al., 2018), we then subtracted this baseline value from original pupil values to analyze four other indices related to phasic pupillary responses (Loewenfeld, 1999; Oster et al., 2022). We calculated pupillary response onset latencies (PROL) that were defined as the time point at which pupillary acceleration reached its maximal and pupillary velocity was negative (i.e. constricting) according to the established criteria (Bergamin and Kardon, 2003). Moreover, we calculated the maximum constriction amplitude, the maximum constriction velocity, and the main sequence slope (pupil peak velocity/amplitude) of the pupillary response. Additionally, we calculated the time of maximum constriction for the time that pupil size reached its maximal constriction (referred to as PeakTime). Regarding saccadic metrics, in addition to SRT, we calculated saccade amplitude (saccade size in degrees), saccade peak velocity (deg/s), the main sequence slope (peak velocity/amplitude), and endpoint accuracy (angular deviation of the end position of the first saccade from the correct saccadic location) to fully understand FEF cTBS time-on-task effects on saccadic metrics as well.

We used a linear mixed model (LMM) to examine the impact of time-on-task (i.e. trial sequence) and the stimulation condition on pupillary and saccadic metrics that allowed us to include these variables as fixed effects, and participants were included as a random intercept, such that fixed biases linked to individuals' traits are included in the model (Pinheiro and Bates, 2000). Moreover, the possible presence of curvature in the relationship between time-on-task and stimulation was assessed by fitting statistical models with one predictor being the square value of the variables of interest following standard techniques (James et al., 2013). Thus, similar to previous pupillometry studies (Hong et al., 2014; Cherng et al., 2021), we included a square function of a fixed factor in linear mixed models to investigate linear and quadratic relationships between time-on-task (trial sequence) and pupillary and saccadic metrics. We reasoned that if cTBS effects became larger after a latency following stimulation, we should observe an optimal value for which the indices exhibit either a maximum or a minimum. Furthermore, to compare the models, we employed the Bayesian information criterion (BIC), which evaluates the goodness of fit by considering the number of parameters involved (Murphy, 2012; Crevecoeur et al., 2017). Our model included the dependent variable y (pupillary and saccadic metrics), and trial sequence (mean-centered: subtracting the mean from every value of a variable) and the square value of trial sequence as fixed predictors, allowing us to interpret trial-to-trial change directly in relation to each individual's own average (Enders and Tofighi, 2007). Three models were used, with Model 1, Model 2, and Model 3, representing linear, quadratic, and both linear and quadratic relationships, respectively. These models examined whether there were linear and quadratic relationships between time-on-task and pupillary or saccadic metrics. LMMs were as follows:

$$\text{Model1}: y = \beta_S + \beta_0 + \beta_1 T$$

$$\text{Model2}: y = \beta_S + \beta_0 + \beta_1 T\text{^}2$$

$$\text{Model3}: y = \beta_S + \beta_0 + \beta_1 T + \beta_2 T\text{^}2$$

Where T is trial sequence (mean-centered), β_S is a random intercept for each participant as an individual offset, and β_0 is a fixed intercept, β_i are the standard coefficients of the statistical model (slopes). The sign of the quadratic term indicates the direction of concavity/convexity (positive sign: U-shaped relationship – convex; negative sign: inverted U-shaped relationship – concave). The model with the lowest BIC value will be chosen as it achieves an optimal balance between explaining the variance in the data and avoiding an excessive number of parameters, and significance is attributed to differences in BIC values greater than 2 (Raftery, 1995). The model produced the highest performance indicated whether there were linear (Model 1), quadratic (Model 2), or linear and quadratic (Model 3) relationships between time-on-task and pupillary or saccadic metrics. Model 4 (linear), Model 5 (quadratic), or Model 6 (linear and quadratic) was then used to examine whether there were linear, quadratic, or both linear and quadratic relationships respectively between time-on-task and pupillary or saccadic metrics in different stimulation conditions according to our theoretical framework:

$$\text{Model4}: y = \beta_S + \beta_0 + \beta_1 T + \beta_2 S + \beta_3 T \times S$$

$$\text{Model5}: y = \beta_S + \beta_0 + \beta_1 T\text{^}2 + \beta_2 S + \beta_3 T\text{^}2 \times S$$

$$\text{Model6}: y = \beta_S + \beta_0 + \beta_1 T + \beta_2 T\text{^}2 + \beta_3 S + \beta_4 T \times S + \beta_5 T\text{^}2 \times S$$

Where T is trial sequence (mean-centered), S is stimulation condition (FEF or vertex). MATLAB (The MathWorks Inc., Natrick, MA, USA) was used for data analysis. All statistical models were performed using R Project (Rstudio Team, 2019; R Core Team, 2020) with the lmer function.

Results

FEF cTBS time-on-task effects on pupillary metrics in the visual-delay task

To investigate time-on-task effects between the FEF and vertex stimulation conditions on PLR metrics, we used LMM to examine whether there were linear and quadratic relationships between time-on-task and pupillary metrics (see Methods). We hypothesized that if there are FEF cTBS time-on-task effects on PLR metrics, then an interaction between trial sequence and the stimulation condition should be observed, exhibiting differences in the time-on-task modulation between the two stimulation conditions. To illustrate time-on-task on PLR metrics (Fig. 2), we sorted trials into 8 time bins according to time-on-task (i.e. trial sequence) in each condition (see Methods). As illustrated in Fig. 2A, baseline pupil size was changed by a time-on-task factor in the visual-delay task. Model 3 exhibited the best performance (Table 1), and thus Model 6 was used to examine whether there were linear and quadratic relationships between time-on-task and baseline pupil size (see Methods). As displayed in Table 2, baseline pupil size decreased linearly over time (Trial: $\beta = -1.11 \times 10^3$, $p = 6.26 \times 10^{-9}$), and an U-shaped relationship was also significant (Trial^2: $\beta = 1.52 \times 10^5$, $p = 3.08 \times 10^{-11}$). Moreover, significantly lower baseline pupil size was observed in the FEF, compared to the vertex stimulation condition (Stim: $p = 1.65 \times 10^{-14}$). A significant interaction between trial sequence and stimulation condition was seen (Trial×Stim: $p = 0.0342$), with reduced decreases in pupil size as a function of trial sequence in the FEF condition (Fig. 3A for model predicted values). As illustrated in Fig. 2B, PROLs increased as trial sequence increased (Trial: $p = 0.00221$). All other effects were not significant. Although peak constriction velocities decreased over time (Fig. 2C, Trial: $p = 6.80 \times 10^{-6}$), and lower peak constriction velocities were obtained with FEF stimulation (Stim: $p = 6.64 \times 10^{-9}$), no significant interaction

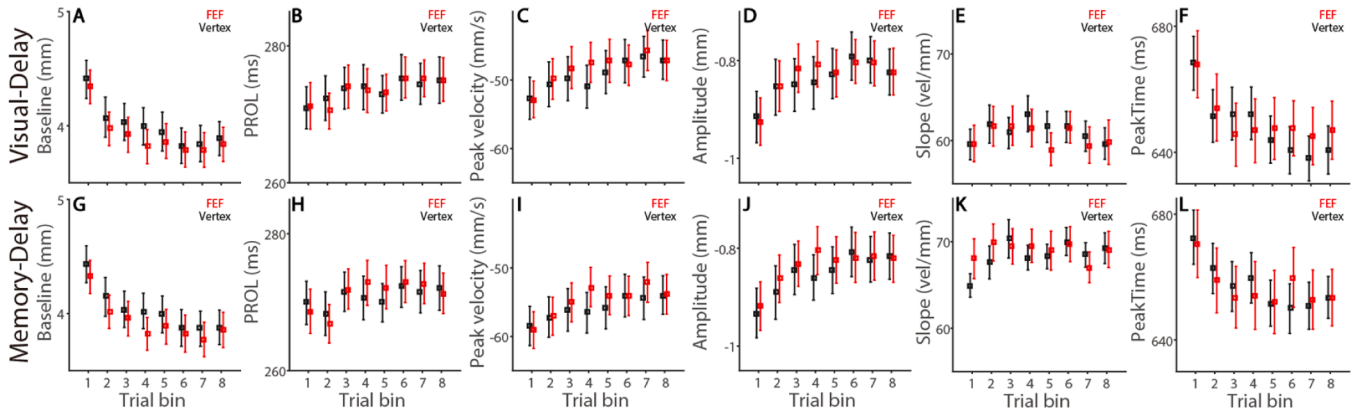

Fig. 2. Time-on-task effects between FEF and vertex cTBS condition on pupillary metrics in the visual-delay and memory-delay saccade task. The squares and error-bars represent the mean values ± standard error across participants. Visual-Delay: visually-guided saccade task. Memory-Delay: memory-guided saccade task. Baseline: baseline pupil size. PROL: pupil response onset latency. Peak Velocity: peak pupil constriction velocity. Amplitude: peak pupil constriction size. Slope: pupil main sequence slope, peak velocity / amplitude. PeakTime: time to peak constriction.

Table 1
Multilevel model for Bayesian information criterion.

Pupil Visual-Delay	BIC					
Model	Baseline	PROL	Peak Velocity	Amplitude	Slope	PeakTime
(1) Y = Trial	8289.077	53,583.91	45,907.39	-3653.301	51,510.22	62,574.34
(2) Y = Trial^2	8634.417	53,623.77	46,127.88	-3564.272	51,505.1	62,755.95
(3) Y = Trial + Trial^2	8080.608	53,609.16	45,915.11	-3702.309	51,522.54	62,543.58
Memory-Delay	BIC					
Model	Baseline	PROL	Peak Velocity	Amplitude	Slope	PeakTime
(1) Y = Trial	8170.811	47,369.23	43,345.26	-3502.46	49,529.53	59,100.59
(2) Y = Trial^2	8559.523	47,411.31	43,507.22	-3398.494	49,528.56	59,179.04
(3) Y = Trial + Trial^2	7996.514	47,381.95	43,336.44	-3550.317	49,543.01	59,062.61

Trial: trial number. Trial^2: trial number squared. Baseline: baseline pupil size. PROL: pupil response onset latency. Peak Velocity: peak pupil constriction velocity. Amplitude: peak pupil constriction size. Slope: peak velocity / amplitude. PeakTime: time to peak constriction. BIC: Bayesian information criterion.

was seen. Constriction amplitude decreased over time (Fig. 2D, Trial: $p = 0.00046$), and an inverted U shaped relationship was also obtained (Trial^2: $p = 2.49 \times 10^{-5}$). Smaller constriction was noted with FEF stimulation (Stim: $p = 2.49 \times 10^{-5}$), and more importantly, a significant interaction between time-on-task and squared trial sequence was seen (Trial^2 ×Stim: $p = 0.01752$), showing a more pronounced U shaped pattern in the FEF stimulation condition (model predicted values: Fig. 3B). No effects were observed in slope analysis (Fig. 2E). As illustrated in Fig. 2F, an U shaped relationship between time-on-task and peak time was seen (Trial^2: $p = 0.000161$), and there was a significant interaction between time-on-task and trial sequence (Trial×Stim: $p = 0.000422$), showing reduced decreases in peak time over time with FEF stimulation (model predicted values: Fig. 3C). In summary, FEF cTBS decreased baseline pupil size, peak constriction velocities and amplitude. Moreover, time-on-task effects in baseline pupil size, constriction amplitude and peak time were also different between the FEF and vertex stimulation conditions.

FEF cTBS time-on-task effects on pupillary metrics in the memory-delay task

In the memory-delay task, we obtained a similar pattern of results. As described in Methods, BIC results (Table 1) were used to evaluate which Model to be used for further analyses (see LMM results in detail in Table 3). As illustrated in Fig. 2G, baseline pupil size linearly decreased as a function of time-on-task (Trial: $\beta = -1.14 \times 10^{3}$, $p = 8.94 \times 10^{-9}$), and an U-shaped relationship was also significant (Trial^2: $\beta = 1.60 \times 10^{5}$, $p = 1.45 \times 10^{-11}$). Furthermore, smaller baseline pupil size was observed with FEF stimulation (Stim: $p = 5.36 \times 10^{-15}$). A significant interaction between trial sequence and stimulation condition was noted (Trial×Stim: $p = 0.0253$), with reduced decreases in pupil size as a function of trial sequence in the FEF condition (model predicted values: Fig. 4A). In addition, the interaction between time-on-task and squared trial sequence was also significant (Trial^2 ×Stim: $p = 0.0264$), showing a more pronounced U shaped pattern in the FEF stimulation condition (model predicted values: Fig. 4B). PROLs increased as trial sequence increased (Fig. 2H: Trial: $p = 1.7 \times 10^{-5}$), and more interestingly, a significant interaction between trial sequence and stimulation condition was seen (Trial×Stim: $p = 0.0266$), with larger time-on-task effects as a function of trial sequence in the FEF condition (model predicted values: Fig. 4C). Peak constriction velocities were modulated by both trial sequence (Fig. 2I: Trial: $p = 6.96 \times 10^{-10}$) and squared trial sequence (Trial^2: $p = 2.80 \times 10^{-10}$), and lower peak constriction velocities were observed with FEF stimulation (Stim: $p = 9.34 \times 10^{-14}$). Moreover, there was a significant interaction between squared trial sequence and stimulation (Trial^2 ×Stim: $p = 4.88 \times 10^{-6}$), showing a pronounced inverted U-shaped pattern with FEF stimulation (model predicted values: Fig. 4D). Constriction amplitude decreased linearly over time (Fig. 2J, Trial: $p = 0.0120$), and an inverted U shaped relationship also obtained (Trial^2: $p = 1.92 \times 10^{-7}$). Smaller constriction amplitude was noted with FEF stimulation (Stim: $p = 9.00 \times 10^{-7}$), and more importantly, the interaction between time-on-task and squared trial sequence was obtained (Trial^2 ×Stim: $p = 0.0161$), showing a more pronounced U shaped pattern in the FEF stimulation condition (model predicted values: Fig. 4E). No effects were observed in slope analysis (Fig. 2K). As illustrated in Fig. 2L, an U shaped relationship between time-on-task and peak time was noted (Trial^2: $p = 0.00852$), and the interaction between time-on-task and trial sequence was

Table 2
Multilevel model for pupillary metrics in the visual-delay task.

Pupil metrics	Visual-delay				
Baseline = Trial + Trial^2 + Stim + Trial*Stim + Trial^2 *Stim (6)					
	Beta estimates	Std. Error	t value	df	p
(Intercept)	3.69E+ 00	1.43E-01	25.825	2.90E+ 01	< 2e-16 * **
Trial	-1.11E-03	1.90E-04	-5.818	6.23E+ 03	6.26e-09 * **
Trial^2	1.52E-05	2.28E-06	6.655	6.23E+ 03	3.08e-11 * **
Stim	1.32E-01	1.71E-02	7.694	6.23E+ 03	1.65e-14 * **
Trial:Stim	-2.54E-04	1.20E-04	-2.118	6.23E+ 03	0.0342 *
Trial^2:Stim	-2.50E-06	1.43E-06	-1.746	6.23E+ 03	0.0809
PROL = Trial + Stim + Trial*Stim (4)					
	Beta estimates	**Std. Error**	**t value**	**df**	**p**
(Intercept)	2.73E+ 02	2.93E+ 00	93.068	2.99E+ 01	< 2e-16 * **
Trial	2.24E-02	7.30E-03	3.061	6.23E+ 03	0.00221 * *
Stim	-4.12E-03	4.36E-01	-0.009	6.23E+ 03	0.99246
Trial:Stim	-5.96E-03	4.60E-03	-1.295	6.23E+ 03	0.19547
Peak Velocity = Trial + Stim + Trial*Stim (4)					
	Beta estimates	**Std. Error**	**t value**	**df**	**p**
(Intercept)	-4.74E+ 01	2.93E+ 00	-16.205	2.78E+ 01	1.07e-15 * **
Trial	1.77E-02	3.93E-03	4.504	6.23E+ 03	6.80e-06 * **
Stim	-1.36E+ 00	2.35E-01	-5.808	6.23E+ 03	6.64e-09 * **
Trial:Stim	9.38E-04	2.48E-03	0.379	6.23E+ 03	0.705
Amplitude = Trial + Trial^2 + Stim + Trial*Stim + Trial^2 *Stim (6)					
	Beta estimates	**Std. Error**	**t value**	**df**	**p**
(Intercept)	-7.82E-01	4.77E-02	-16.404	2.98E+ 01	< 2e-16 * **
Trial	2.62E-04	7.47E-05	3.505	6.23E+ 03	0.00046 * **
Trial^2	-4.64E-06	8.95E-07	-5.188	6.23E+ 03	2.20e-07 * **
Stim	-2.84E-02	6.73E-03	-4.219	6.23E+ 03	2.49e-05 * **
Trial:Stim	2.93E-05	4.71E-05	0.624	6.23E+ 03	0.53291
Trial^2:Stim	1.34E-06	5.63E-07	2.376	6.23E+ 03	0.01752 *
Slope = Trial^2 + Stim + Trial^2 *Stim (5)					
	Beta estimates	**Std. Error**	**t value**	**df**	**p**
(Intercept)	6.02E+ 01	1.87E+ 00	32.189	4.38E+ 01	< 2e-16 * **
Trial^2	5.33E-07	7.42E-05	0.007	6.23E+ 03	0.994
Stim	8.90E-01	5.57E-01	1.596	6.23E+ 03	0.111
Trial^2:Stim	-6.19E-05	4.66E-05	-1.327	6.23E+ 03	0.185
PeakTime = Trial + Trial^2 + Stim + Trial*Stim + Trial^2 *Stim (6)					
	Beta estimates	**Std. Error**	**t value**	**df**	**p**
(Intercept)	6.45E+ 02	8.25E+ 00	78.199	3.08E+ 01	< 2e-16 * **
Trial	-2.21E-02	1.49E-02	-1.483	6.23E+ 03	0.138052
Trial^2	6.73E-04	1.78E-04	3.776	6.23E+ 03	0.000161 * **
Stim	5.10E-01	1.34E+ 00	0.381	6.23E+ 03	0.703302
Trial:Stim	-3.31E-02	9.37E-03	-3.528	6.23E+ 03	0.000422 * **
Trial^2:Stim	-1.65E-04	1.12E-04	-1.47	6.23E+ 03	0.141514

Trial: trial number. Trial^2: trial number squared. Stim: stimulation condition. Baseline: baseline pupil size. PROL: pupil response onset latency. Peak Velocity: peak pupil constriction velocity. Amplitude: peak pupil constriction size. Slope: peak velocity/amplitude. PeakTime: time to peak constriction. Std. Error: standard error. df: degree of freedom. p: p value. *p < .05; * *p < . 01; * **p < . 001.

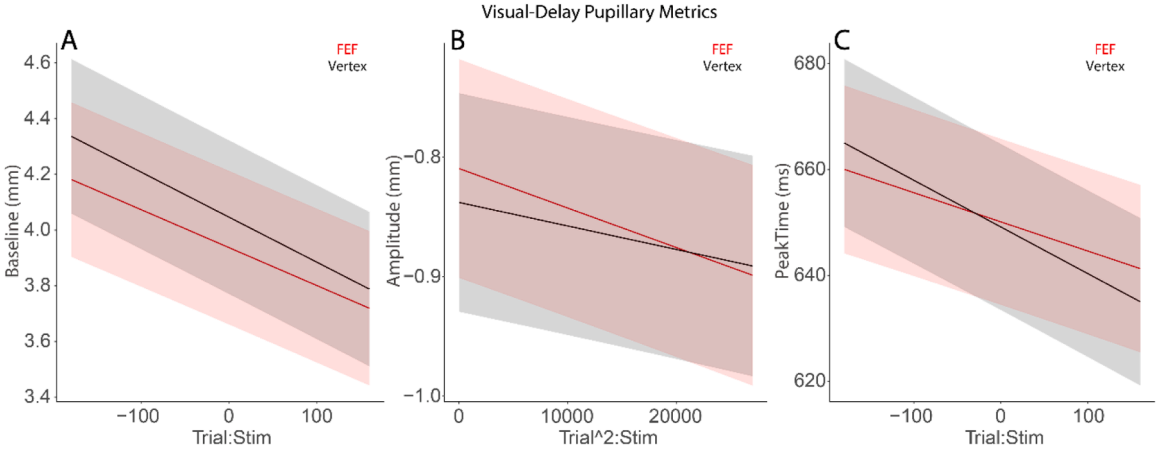

Fig. 3. Model predicted best fit lines for the interaction effect between trial and stimulation in the visual-delay task. (A) Interaction effects between trial sequence and stimulation on baseline pupil size. (B) Interaction effects between trial sequence squared and stimulation on amplitude. (C) Interaction effects between trial sequence and stimulation on peak time. The shaded colored regions surrounding the predicted lines represent the ± 95% confidence interval for different conditions. Baseline: baseline pupil size. Amplitude: peak pupil constriction size.

Table 3
Multilevel model for pupillary metrics in the memory-delay task.

Pupil metrics	Memory-delay				
Baseline = Trial + Trial^2 + Stim + Trial*Stim + Trial^2 *Stim (6)					
	Beta estimates	Std. Error	t value	df	p
(Intercept)	3.70E+ 00	1.41E-01	26.173	2.93E+ 01	< 2e-16 * **
Trial	-1.14E-03	1.98E-04	-5.758	5.95E+ 03	8.94e-09 * **
Trial^2	1.60E-05	2.36E-06	6.766	5.95E+ 03	1.45e-11 * **
Stim	1.41E-01	1.80E-02	7.839	5.95E+ 03	5.36e-15 * **
Trial:Stim	-2.79E-04	1.25E-04	-2.237	5.95E+ 03	0.0253 *
Trial^2: Stim	-3.31E-06	1.49E-06	-2.221	5.95E+ 03	0.0264 *
PROL = Trial + Stim + Trial*Stim (4)					
	Beta estimates	Std. Error	t value	df	p
(Intercept)	2.71E+ 02	2.94E+ 00	92.191	2.86E+ 01	< 2e-16 * **
Trial	2.32E-02	5.39E-03	4.305	5.95E+ 03	1.7e-05 * **
Stim	-2.72E-01	3.24E-01	-0.838	5.95E+ 03	0.402
Trial:Stim	-7.53E-03	3.40E-03	-2.217	5.95E+ 03	0.0266 *
Peak Velocity = Trial + Trial^2 + Stim + Trial*Stim + Trial^2 *Stim (6)					
	Beta estimates	Std. Error	t value	df	p
(Intercept)	-5.13E+ 01	2.85E+ 00	-17.988	2.91E+ 01	< 2e-16 * **
Trial	2.35E-02	3.81E-03	6.177	5.95E+ 03	6.96e-10 * **
Trial^2	-2.88E-04	4.56E-05	-6.32	5.95E+ 03	2.80e-10 * **
Stim	-2.60E+ 00	3.48E-01	-7.468	5.95E+ 03	9.34e-14 * **
Trial:Stim	-4.49E-03	2.40E-03	-1.867	5.95E+ 03	0.062
Trial^2: Stim	1.32E-04	2.87E-05	4.574	5.95E+ 03	4.88e-06 * **
Amplitude = Trial + Trial^2 + Stim + Trial*Stim + Trial^2 *Stim (6)					
	Beta estimates	Std. Error	t value	df	p
(Intercept)	-7.83E-01	4.76E-02	-16.433	3.00E+ 01	< 2e-16 * **
Trial	1.90E-04	7.56E-05	2.513	5.95E+ 03	0.0120 *
Trial^2	-4.71E-06	9.04E-07	-5.213	5.95E+ 03	1.92e-07 * **
Stim	-3.39E-02	6.89E-03	-4.917	5.95E+ 03	9.00e-07 * **
Trial:Stim	8.78E-05	4.77E-05	1.842	5.95E+ 03	0.0655
Trial^2: Stim	1.37E-06	5.70E-07	2.406	5.95E+ 03	0.0161 *
Slope = Trial^2 + Stim + Trial^2 *Stim (5)					
	Beta estimates	Std. Error	t value	df	p
(Intercept)	6.95E+ 01	1.73E+ 00	40.123	5.22E+ 01	< 2e-16 * **
Trial^2	-2.70E-05	7.74E-05	-0.349	5.95E+ 03	0.727
Stim	-1.45E-01	5.90E-01	-0.246	5.95E+ 03	0.806
Trial^2: Stim	-4.41E-05	4.88E-05	-0.904	5.95E+ 03	0.366
PeakTime = Trial + Trial^2 + Stim + Trial*Stim + Trial^2 *Stim (6)					
	Beta estimates	Std. Error	t value	df	p
(Intercept)	6.53E+ 02	8.27E+ 00	78.894	3.06E+ 01	< 2e-16 * **
Trial	-8.99E-03	1.43E-02	-0.629	5.95E+ 03	0.52916
Trial^2	4.50E-04	1.71E-04	2.632	5.95E+ 03	0.00852 * *
Stim	7.09E-01	1.30E+ 00	0.544	5.95E+ 03	0.58643
Trial:Stim	-2.89E-02	9.01E-03	-3.207	5.95E+ 03	0.00135 * *
Trial^2: Stim	-1.14E-05	1.08E-04	-0.105	5.95E+ 03	0.91609

Trial: trial number. Trial^2: trial number squared. Stim: stimulation condition. Baseline: baseline pupil size. PROL: pupil response onset latency. Peak Velocity: peak pupil constriction velocity. Amplitude: peak pupil constriction size. Slope: peak velocity / amplitude. PeakTime: time to peak constriction. Std. Error: standard error. df: degree of freedom. p: p value. *p < .05; * *p < . 01; * **p < . 001.

observed (Trial×Stim: $p = 0.00135$), showing reduced decreases in peak time over time with FEF stimulation (model predicted values: Fig. 4F). In general, FEF cTBS decreased baseline pupil size, peak constriction velocities and amplitude. Moreover, time-on-task effects in baseline pupil size, PROL, peak velocity, amplitude and peak time were also different between the FEF and vertex stimulation conditions.

FEF cTBS time-on-task effects on saccadic metrics in the visual-delay and memory-delay task

We also systematically examined time-on-task effects between the FEF and vertex stimulation conditions on saccadic metrics. Similarly, we sorted trials into 8 time bins according to time-on-task in each condition to illustrate time-on-task on saccadic metrics (Fig. 5), and BIC was used to select which model for subsequent analysis (Table 4). In visually-guided saccades analysis, detailed values of LMM are displayed in Table 5. As illustrated in Fig. 5A, SRTs decreased linearly over time (Trial: $p = 1.11 \times 10^{-11}$), and longer SRTs were obtained with FEF stimulation (Stim: $p = 7.39 \times 10^{-10}$). Furthermore, a more pronounced time-on-task effect was observed with FEF stimulation (Trial×Stim: $p = 0.000106$; model predicted values: Fig. 6A). Saccadic peak velocities decreased with time (Fig. 5B: Trial: $p = 0.01441$), and an U-shaped pattern was also noted (Trial^2: $p = 0.00581$). Moreover, significantly lower peak velocities were obtained with FEF stimulation (Stim: $p = 0.02351$). All other effects were not significant. No effects were obtained in amplitude and slope analyses (amplitude: Fig. 5C; slope: Fig. 5D). As illustrated in Fig. 5E, larger endpoint deviation was obtained with FEF stimulation (Stim: $p = 9.53 \times 10^{-5}$).

In memory-guided saccades, as expected, there were lower saccade peak velocities and larger endpoint deviation, compared to visually-guided saccades (Fig. 5). Detail values of LMM are displayed in Table 6. There were no effects in SRTs (Fig. 5F). As illustrated in Fig. 5G, an U-shaped pattern in saccadic peak velocities was also seen (Trial^2: $p = 0.00927$). Moreover, time-on-task effects in the linear fashion in peak velocity were reduced with FEF stimulation (Trial×Stim: $p = 0.03766$; model predicted values: Fig. 6B). For saccade amplitude (Fig. 5H), the interaction between time-on-task and trial sequence was also significant (Trial×Stim: $p = 0.0218$), with different directions of time-on-task effects (model predicted values: Fig. 6C). No effects were observed in the main sequence slope analysis (Fig. 5I). Larger endpoint deviation was obtained with FEF stimulation (Fig. 5J: Stim: $p = 0.000338$). Overall, FEF cTBS effects and its time-on-task effects were weaker in saccadic metrics.

Discussion

To investigate the time-on-task effects on pupillary and saccadic metrics following FEF cTBS, we analyzed the dynamics of pupillary light reflex elicited by a bright stimulus in both the visual-delay and memory-delay saccade tasks following application of cTBS over the right FEF and the vertex. FEF cTBS had an impact on PLR metrics, resulting in decreased baseline pupil size, peak constriction velocities, and constriction amplitude. Importantly, we observed differences in time-on-task effects between the FEF and vertex stimulation conditions for baseline pupil size, constriction amplitude, and peak time in both tasks. Additionally, while some saccadic metrics showed differences in time-on-task effects between the FEF and vertex conditions, these differences were less pronounced. Overall, our findings demonstrate distinct time-on-task effects on pupillary metrics for the FEF and vertex cTBS conditions. These results suggest that the duration of the effects after FEF cTBS varies among pupillary metrics and emphasize the value of analyzing pupillary metrics to gain insights into the impact of cTBS on

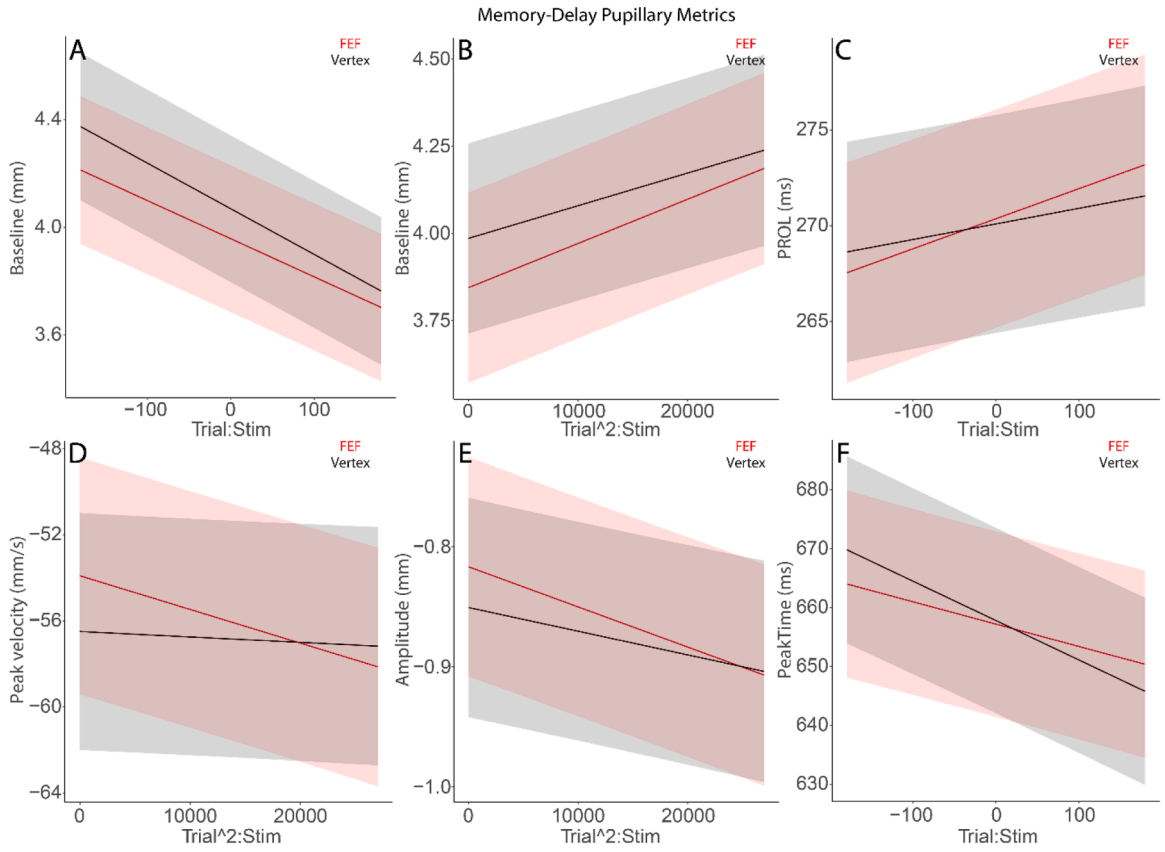

Fig. 4. Model predicted best fit lines for the interaction effect between trial and stimulation in the memory-delay task. (A) Interaction effects between trial sequence and stimulation on baseline pupil size. (B) Interaction effects between trial sequence squared and stimulation on amplitude. (C) Interaction effects between trial sequence and stimulation on PROL. (D) Interaction effects between trial sequence squared and stimulation on peak velocity. (E) Interaction effects between trial sequence squared and stimulation on amplitude. (F) Interaction effects between trial sequence and stimulation on peak time. The shaded colored regions surrounding the predicted lines represent the ± 95 % confidence interval for different conditions. Baseline: baseline pupil size. PROL: pupil response onset latency. Peak Velocity: peak pupil constriction velocity. Amplitude: peak pupil constriction size. Slope: peak velocity / amplitude. PeakTime: time to peak constriction.

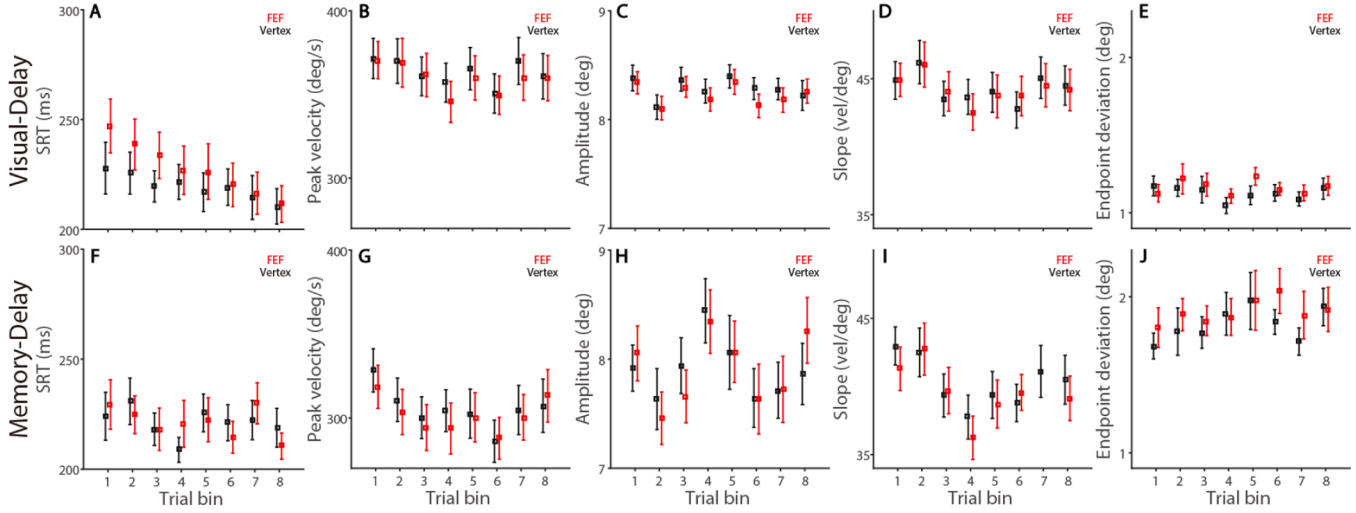

Fig. 5. Time-on-task effects between FEF and vertex cTBS condition on visually- and memory-guided saccadic metrics. The squares and error-bars represent the mean values ± standard error across participants. Visual-Delay: visually-guided saccade task. Memory-Delay: memory-guided saccade task. SRT: saccade reaction time. Peak velocity: saccade peak velocity. Amplitude: saccade amplitude. Slope: peak velocity / amplitude. Endpoint: saccade endpoint deviation.

human behavior.

Control of pupillary light reflex responses

The measurement of pupillary kinematics is important for understanding the control of pupil size and the underlying mechanisms of this

Table 4
Multilevel model for Bayesian information criterion.

Saccade Visual-Delay	BIC				
Model	SRT	PeakVel	Amp	Slope	Endpoint
(1) Y = Trial	69,333.87	68,026.13	19,711.66	43,639.29	13,776.72
(2) Y = Trial^2	69,438.24	68,002.61	19,715.21	43,639.19	13,783.7
(3) Y = Trial + Trial^2	69,358.38	67,990.55	19,739.2	43,643.53	13,808.58
Memory-Delay	BIC				
Model	SRT	PeakVel	Amp	Slope	Endpoint
(1) Y = Trial	68,657.49	67,796.32	23,858.75	97,599.7	19,840.52
(2) Y = Trial^2	68,673.07	67,767.13	23,866.44	97,609.5	19,853.16
(3) Y = Trial + Trial^2	68,682.21	67,743.49	23,889.98	97,619.66	19,871.1

Trial: trial number. Trial^2: trial number squared. SRT: saccade reaction time. PeakVel: saccade peak velocity. Amp: saccade amplitude. Slope: peak velocity / amplitude. Endpoint: endpoint deviation. BIC: Bayesian information criterion.

Table 5
Multilevel model for saccadic metrics in the visual-delay task.

Saccade metrics	Visual-delay				
SRT= Trial + Stim + Trial*Stim (4)					
	Beta estimates	Std. Error	t value	df	p
(Intercept)	2.37E+ 02	8.23E+ 00	28.849	3.18E+ 01	< 2e-16 * **
Trial	-1.74E-01	2.56E-02	-6.804	6.23E+ 03	1.11e-11 * **
Stim	-9.43E+ 00	1.53E+ 00	-6.167	6.23E+ 03	7.39e-10 * **
Trial:Stim	6.26E-02	1.61E-02	3.878	6.23E+ 03	0.000106 * **
PeakVel = Trial + Trial^2 + Stim + Trial*Stim + Trial^2 *Stim (6)					
	Beta estimates	Std. Error	t value	df	p
(Intercept)	3.51E+ 02	1.22E+ 01	28.785	3.12E+ 01	< 2e-16 * **
Trial	-5.63E-02	2.30E-02	-2.448	6.23E+ 03	0.01441 *
Trial^2	7.60E-04	2.76E-04	2.759	6.23E+ 03	0.00581 * *
Stim	4.69E+ 00	2.07E+ 00	2.266	6.23E+ 03	0.02351 *
Trial:Stim	1.15E-02	1.45E-02	0.795	6.23E+ 03	0.42664
Trial^2: Stim	-5.30E-05	1.73E-04	-0.306	6.23E+ 03	0.75972
Amp = Trial + Stim + Trial*Stim (4)					
	Beta estimates	Std. Error	t value	df	p
(Intercept)	8.16E+ 00	1.02E-01	79.755	4.05E+ 01	< 2e-16 * **
Trial	-2.70E-04	4.89E-04	-0.551	6.23E+ 03	5.81E-01
Stim	5.45E-02	2.92E-02	1.866	6.23E+ 03	6.21E-02
Trial:Stim	1.09E-04	3.08E-04	0.354	6.23E+ 03	7.24E-01
Slope = Trial^2 + Stim + Trial^2 *Stim (5)					
	Beta estimates	Std. Error	t value	df	p
(Intercept)	4.41E+ 01	1.45E+ 00	30.357	3.34E+ 01	< 2e-16 * **
Trial^2	4.75E-05	3.95E-05	1.202	6.23E+ 03	0.229
Stim	6.72E-02	2.97E-01	0.226	6.23E+ 03	0.821
Trial^2: Stim	9.98E-06	2.48E-05	0.402	6.23E+ 03	0.688
Endpoint = Trial + Stim + Trial*Stim (4)					
	Beta estimates	Std. Error	t value	df	p
(Intercept)	1.27E+ 00	5.77E-02	21.975	4.46E+ 01	< 2e-16 * **
Trial	1.69E-04	3.04E-04	0.555	6.23E+ 03	0.579
Stim	-7.09E-02	1.82E-02	-3.905	6.23E+ 03	9.53e-05 * **
Trial:Stim	-1.59E-04	1.92E-04	-0.83	6.23E+ 03	0.407

Trial: trial number. Trial^2: trial number squared. Stim: stimulation condition. SRT: saccade reaction time. PeakVel: saccade peak velocity. Amp: saccade amplitude. Slope: peak velocity / amplitude. Endpoint: endpoint deviation. Std. Error: standard error. df: degree of freedom. p: p value. *p < .05; * *p < . 01; * **p < . 001.

control (Loewenfeld, 1999). For example: as noted by Loewenfeld (1999), pupil response onset latency, similar to the visual evoked potential, could objectively reflect delays in visual processing. Because pupillary response amplitude is subject to the mechanical properties of the iris, PROL could provide a more accurate assessment of afferent input to the eyes (Loewenfeld, 1999; Bergamin and Kardon, 2003). Indeed, previous studies have shown that pupillary metrics are informative in elucidating pupil modulation by various visual and cognitive processes (Steinhauer and Hakerem, 1992; Barbur, 2004; Yu et al., 2007; Oster et al., 2022), and they can provide important insights for clinical investigations (Kardon, 1995; Prettyman et al., 1997; Frost et al., 2013, 2017; Hall and Chilcott, 2018; Oh et al., 2019; Van Stavern et al., 2019; Kawasaki et al., 2020).

The circuit involved in the PLR includes several brain areas (McDougal and Gamlin, 2015; May et al., 2019). The pretectal olivary nucleus (PON) receives direct retinal inputs and has direct projections to the preganglionic subdivision of the Edinger–Westphal nucleus (EWpg), which connects to postganglionic motoneurons in the ciliary ganglion that supply the intraocular muscles of the eye. Microstimulation of the PON or EW evokes pupillary constriction with a latency of approximately 100 ms after stimulation in behaving monkeys (Gamlin et al., 1995; Gamlin, 2000; Pong and Fuchs, 2000). Luminance-sensitive neurons have also been identified in the PON (Gamlin et al., 1995; Pong and Fuchs, 2000; Clarke et al., 2003) and EW (Gamlin, 2000), showing that these luminance neurons exhibit the characteristics appropriate for mediating the PLR. However, it should be noted that the luminance neurons in the PON are more closely correlated with visual stimulus properties rather than directly influencing the metrics of subsequent PLR responses (Pong and Fuchs, 2000). These results suggest that PLR metrics are likely coordinated more closely by the EWpg, and other inputs beyond the PON are needed to contribute to PLR kinematics. The EW receives important control signals from other structures, and the locus coeruleus (LC) could possibly have a direct or indirect connection to the EW (Joshi and Gold, 2020), although the anatomical connection has yet to be clearly established. The LC is thus potentially involved in affecting pupil size. Additionally, the EW receives projections from the SC directly and indirectly via the central mesencephalic reticular formation (Grantyn and Grantyn, 1982; Scudder et al., 1996; May, 2006; May et al., 2016; Bohlen et al., 2017). As mentioned, the intermediate/deep layers of the SC (SCi) anatomically and physiologically connects to the FEF (Komatsu and Suzuki, 1985; Segraves and Goldberg, 1987; Stanton et al., 1988; Schlag-Rey et al., 1992; Everling and Munoz, 2000; Sommer and Wurtz, 2000), and this circuit plays a causal role in the control of orienting responses including eye/head/body movement, attention shifts and pupil dilation (Hess et al., 1946; Akert, 1949; Sokolov, 1963; Corneil and Munoz, 2014). The EW could integrate these important signals to coordinate PLR metrics.

FEF cTBS effects on pupillary and saccadic metrics

PLR metrics were modulated by FEF cTBS. Smaller baseline pupil sizes, peak constriction velocities, and amplitude were observed in the FEF condition compared to the vertex condition. These results are consistent with our previous study, which showed reduced constriction amplitude after FEF cTBS (Hsu et al., 2022). However, our previous study did not find differences between baseline pupil size between the two stimulation conditions, possibly attributing to using LMM here to increase the statistical power of the analysis on baseline pupil size. Importantly, time-on-task effects were different between the FEF and vertex conditions, showing reduced baseline time-on-task effects and different non-linear relationships in amplitude and peak time between the two stimulation conditions in both tasks. These results suggest that FEF cTBS modulates time-on-task effects on pupillary metrics.

What are the neural mechanisms underlying the effects of FEF cTBS on pupillary metrics? There are two possibilities. First, the FEF has direct connections to the pretectal nucleus (Künzle and Akert, 1977; Leichnetz,

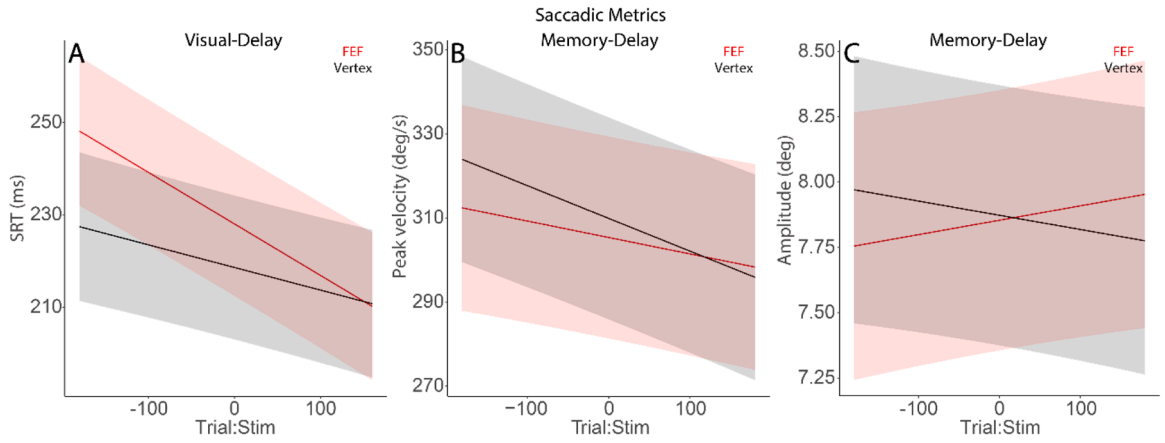

Fig. 6. Model predicted best fit lines for the interaction effect between trial and stimulation for saccadic metrics. (A) Interaction effects between trial sequence and stimulation on SRT in the visual-delay task. (B) Interaction effects between trial sequence squared and stimulation on peak velocity in the memory-delay task. (C) Interaction effects between trial sequence and stimulation on amplitude in the memory-delay task. The shaded colored regions surrounding the predicted lines represent the ± 95% confidence interval for different conditions. SRT: saccade reaction time. Peak velocity: saccade peak velocity. Amplitude: saccade amplitude.

Table 6
Multilevel model for saccadic metrics in the memory-delay task.

Saccade metrics	Memory-delay				
SRT= Trial + Stim + Trial*Stim (4)					
	Beta estimates	Std. Error	t value	df	p
(Intercept)	2.22E+ 02	7.57E+ 00	29.314	3.72E+ 01	< 2e-16 * **
Trial	-5.26E-02	3.21E-02	-1.637	5.95E+ 03	0.102
Stim	-5.69E-01	1.93E+ 00	-0.294	5.95E+ 03	0.768
Trial:Stim	1.72E-02	2.03E-02	0.85	5.95E+ 03	0.395
PeakVel = Trial + Trial^2 + Stim + Trial*Stim + Trial^2 *Stim (6)					
	Beta estimates	Std. Error	t value	df	p
(Intercept)	2.92E+ 02	1.29E+ 01	22.652	3.38E+ 01	< 2e-16 * **
Trial	-3.48E-04	2.96E-02	-0.012	5.95E+ 03	0.99062
Trial^2	9.21E-04	3.54E-04	2.603	5.95E+ 03	0.00927 * *
Stim	4.13E+ 00	2.70E+ 00	1.532	5.95E+ 03	0.12546
Trial:Stim	-3.88E-02	1.87E-02	-2.079	5.95E+ 03	0.03766 *
Trial^2: Stim	4.49E-05	2.23E-04	0.201	5.95E+ 03	0.8405
Amp = Trial + Stim + Trial*Stim (4)					
	Beta estimates	Std. Error	t value	df	p
(Intercept)	7.84E+ 00	2.62E-01	29.902	3.11E+ 01	< 2e-16 * **
Trial	1.64E-03	7.55E-04	2.176	5.95E+ 03	.0296 *
Stim	1.87E-02	4.54E-02	0.411	5.95E+ 03	6.81E-01
Trial:Stim	-1.09E-03	4.76E-04	-2.295	5.95E+ 03	0.0218 *
Slope = Trial + Stim + Trial*Stim (4)					
	Beta estimates	Std. Error	t value	df	p
(Intercept)	8.42E+ 01	3.49E+ 01	2.416	1.98E+ 03	0.0158 *
Trial	4.90E-01	3.64E-01	1.343	5.97E+ 03	0.1793
Stim	-2.15E+ 01	2.19E+ 01	-0.982	5.97E+ 03	0.3263
Trial:Stim	-2.49E-01	2.30E-01	-1.082	5.96E+ 03	0.2791
Endpoint = Trial + Stim + Trial*Stim (4)					
	Beta estimates	Std. Error	t value	df	p
(Intercept)	2.03E+ 00	1.10E-01	18.526	4.19E+ 01	< 2e-16 * **
Trial	1.99E-04	5.40E-04	0.368	5.95E+ 03	0.713253
Stim	-1.17E-01	3.25E-02	-3.586	5.95E+ 03	0.000338 * **
Trial:Stim	1.46E-04	3.41E-04	0.428	5.95E+ 03	0.668552

Trial: trial number. Trial^2: trial number squared. Stim: stimulation condition. SRT: saccade reaction time. PeakVel: saccade peak velocity. Amp: saccade amplitude. Slope: peak velocity/amplitude. Endpoint: endpoint deviation. Std. Error: standard error. df: degree of freedom. p: p value. *p < .05; * *p < . 01; * **p < . 001.

1982; Huerta et al., 1986; Stanton et al., 1988). However, it is less likely that the FEF-PON pathway underlies the observed modulation, as the EW possibly plays a more important role in controlling PLR metrics. An alternative pathway through the FEF-SCi-EW may affect PLR metrics. Research in behaving monkeys has shown that this pathway is causally involved in mediating pupillary luminance responses modulated by high-level functions such as attention (Ebitz and Moore, 2017; Wang and Munoz, 2018), suggesting a central role of this pathway in mediating high-level PLR responses.

Saccadic and pupillary responses have been correlated in previous research (e.g., Wang et al., 2015; Dalmaso et al., 2020), and this coordination is likely mediated by the oculomotor circuit (Lehmann and Corneil, 2016; Ebitz and Moore, 2017; Wang and Munoz, 2021,2023). Therefore, FEF cTBS should also affect saccadic responses. However, we did not observe reliable effects of FEF cTBS on saccadic metrics, although some differences were noted. These results are generally consistent with previous studies showing that the effects of FEF cTBS on saccadic responses are highly variable and task-dependent (Nyffeler et al., 2006c, b, a; Cameron et al., 2015; Gurel et al., 2018; Hsu et al., 2021). Due to the gating role of omnipause neurons in the brainstem (e.g., Scudder et al., 2002), signals must surpass a threshold to evoke saccades. Therefore, saccades may be less sensitive to small disruptions, which could explain the weaker effects of FEF cTBS on saccadic metrics. In summary, we argue that the FEF-SCi-EW pathway likely underlies the observed effects of FEF cTBS on pupillary metrics.

Limitations and future directions

The current paradigm allowed us to investigate the time-on-task modulation between the FEF and vertex cTBS conditions. However, the stimulus-location conditions were collapsed to increase the statistical power for time-on-task analysis. Therefore, the study is limited to comparing the time-on-task effects when the stimulus was presented at the location aligned or unaligned with the location of saccade planning and working memory. Future work would benefit from simplifying the stimulus conditions to increase statistical power for further explorations in this line of research. Additionally, although our work suggested an interaction between time-on-task and stimulation in pupillary metrics, we observed a linear or quadratic interaction. Future work is needed to more comprehensively explore both linear and non-linear time-on-task effects. Furthermore, this study is limited by relatively small sample sizes, although the sample size is sufficient to demonstrate the effects of MRI-guided TMS stimulation (Sack et al., 2009). The sub-optimal localization of FEF in some participants was inevitable due to

individual differences. The gold standard localization of FEF locations with fMRI (Sack et al., 2009) is certainly an important consideration to address this research question. In summary, the time-on-task effects between the FEF and vertex stimulation conditions were particularly different in pupillary metrics, suggesting that FEF cTBS effects change over time. Moreover, pupillary metrics were more sensitive to FEF cTBS effects compared to saccadic metrics. Further investigation focusing on pupillary metrics is important to examine the sensitivity of using pupillary responses as an index to understand the effects of TMS stimulation on human performance.

Declaration of Competing Interest

The authors report no conflicts of interest.

Data availability

Data are available from the authors upon reasonable request following publication.

Acknowledgments

This work was supported by grants from Taiwan National Science and Technology Council (110–2636-H-008–004, 111–2628-H-008–003 and 112–2628-H-038–001) to CW and (110–2410-H-008–040-MY3) to NM, and Taipei Medical University (TMU112-AE1-B12) to CW.

Credit Author Statement

All authors contributed to the study conception; C.W. analyzed data and wrote the first draft of the manuscript. All authors provided comments and edits on various drafts of the manuscript.

References

Akert, K., 1949. Der visuelle Greifreflex. Helv. Physiol. Pharmacol. Acta 7, 112–134.
Barbur, J., 2004. Learning from the pupil-studies of basic mechanisms and clinical applications. In: Chalupa, L.M., Werner, J.S. (Eds.), The Visual Neurosciences. MIT Press, Cambridge, MA, pp. 641–656.
Bartolomeo, P., Seidel Malkinson, T., 2019. Hemispheric lateralization of attention processes in the human brain. Curr. Opin. Psychol. 29.
Bergamin, O., Kardon, R.H., 2003. Latency of the pupil light reflex: sample rate, stimulus intensity, and variation in normal subjects. Investig. Ophthalmol. Vis. Sci. 44, 1546–1554.
Binda, P., Gamlin, P.D., 2017. Renewed attention on the pupil light reflex. Trends Neurosci. 40, 455–457 (Available at). ⟨http://linkinghub.elsevier.com/retrieve/pii/S0166223617301224⟩.
Binda, P., Murray, S.O., 2015. Keeping a large-pupilled eye on high-level visual processing. Trends Cogn. Sci. 19, 1–3 (Available at). ⟨http://www.ncbi.nlm.nih.gov/pubmed/25467128⟩.
Bohlen, M.O., Warren, S., May, P.J., 2017. A central mesencephalic reticular formation projection to medial rectus motoneurons supplying singly and multiply innervated extraocular muscle fibers. J. Comp. Neurol. 525, 2000–2018 (Available at). ⟨http://www.ncbi.nlm.nih.gov/pubmed/28177529⟩.
Cameron, I.G.M., Riddle, J.M., D'Esposito, M., 2015. Dissociable roles of dorsolateral prefrontal cortex and frontal eye fields during saccadic eye movements. Front. Hum. Neurosci. 9, 613.
Chen, J.-T., Kuo, Y.-C., Hsu, T.-Y., Wang, C.-A., 2022. Fatigue and arousal modulations revealed by saccade and pupil dynamics. Int. J. Environ. Res. Public Health 19. ⟨https://www.mdpi.com/1660-4601/19/15/9234/htm⟩.
Cherng, Y.G., Crevecoeur, F., Wang, C.A., 2021. Effects of pupillary light and darkness reflex on the generation of pro- And anti-saccades. Eur. J. Neurosci. 53, 1769–1782. ⟨https://onlinelibrary.wiley.com/doi/10.1111/ejn.15083⟩.
Cherng, Y.-G., Baird, T., Chen, J.-T., Wang, C.-A., 2020. Background luminance effects on pupil size associated with emotion and saccade preparation. Sci. Rep. 10, 15718. ⟨http://www.nature.com/articles/s41598-020-72954-z⟩.
Clarke, R.J., Zhang, H., Gamlin, P.D.R., 2003. Primate pupillary light reflex: receptive field characteristics of pretectal luminance neurons. J. Neurophysiol. 89, 3168–3178. ⟨http://www.ncbi.nlm.nih.gov/pubmed/12611972⟩.
R. Core Team , 2020. R Core Team (2020). R: A language and environment for statistical computing. R Foundation for Statistical Computing, Vienna, Austria. URL https://www.R-project.org/.
Corneil, B.D., Munoz, D.P., 2014. Overt responses during covert orienting. Neuron 82, 1230–1243.
Crevecoeur, F., Barrea, A., Libouton, X., Thonnard, J.-L.L., Lefèvre, P., 2017. Multisensory components of rapid motor responses to fingertip loading. J. Neurophysiol. 118, 331–343. ⟨https://www.physiology.org/doi/10.1152/jn.00091.2017⟩.
Dalmaso, M., Castelli, L., Galfano, G., 2020. Microsaccadic rate and pupil size dynamics in pro-/anti-saccade preparation: the impact of intermixed vs. blocked trial administration. Psychol. Res. 84, 1320–1332 (Available at). ⟨https://link.springer.com/article/10.1007/s00426-018-01141-7⟩.
Ebitz, R.B., Moore, T., 2017. Selective modulation of the pupil light reflex by microstimulation of prefrontal cortex. J. Neurosci. 37, 5008–5018 (Available at). ⟨http://www.jneurosci.org/lookup/doi/10.1523/JNEUROSCI.2433-16.2017⟩.
Enders, C.K., Tofighi, D., 2007. Centering predictor variables in cross-sectional multilevel models: a new look at an old issue. Psychol. Methods 12.
Everling, S., Munoz, D.P., 2000. Neuronal correlates for preparatory set associated with pro-saccades and anti-saccades in the primate frontal eye field. J. Neurosci. 20, 387–400.
Frost, S., Kanagasingam, Y., Sohrabi, H., Taddei, K., Bateman, R., Morris, J., Benzinger, T., Goate, A., Masters, C., Martins, R., 2013. Pupil response biomarkers distinguish amyloid precursor protein mutation carriers from non-carriers. Curr. Alzheimer Res. 10.
Frost, S., Robinson, L., Rowe, C.C., Ames, D., Masters, C.L., Taddei, K., Rainey-Smith, S. R., Martins, R.N., Kanagasingam, Y., 2017. Evaluation of cholinergic deficiency in preclinical Alzheimer's disease using pupillometry. J. Ophthalmol. 2017.
Gamlin, P., 2000. Functions of the edinger-westphal nucleus. In: Burnstock, G., Sillito, A. (Eds.), Nervous Control of the Eye. Harwood Academic, Amsterdam, pp. 117–154.
Gamlin, P.D., Zhang, H., Clarke, R.J., 1995. Luminance neurons in the pretectal olivary nucleus mediate the pupillary light reflex in the rhesus monkey. Exp. Brain Res. 106, 169–176 (Available at). ⟨http://www.ncbi.nlm.nih.gov/pubmed/8542972⟩.
Gandhi, N.J., Katnani, H.A., 2011. Motor functions of the superior colliculus. Annu Rev. Neurosci. 34, 205–231.
Grantyn, A., Grantyn, R., 1982. Axonal patterns and sites of termination of cat superior colliculus neurons projecting in the tecto-bulbo-spinal tract. Exp. Brain Res. 46, 243–256 (Available at). ⟨http://www.ncbi.nlm.nih.gov/pubmed/7095033⟩.
Gurel, S.C., Castelo-Branco, M., Sack, A.T., Duecker, F., 2018. Assessing the functional role of frontal eye fields in voluntary and reflexive saccades using continuous theta burst stimulation. Front. Neurosci. 12, 944 (Available at). ⟨https://www.frontiersin.org/article/10.3389/fnins.2018.00944/full⟩.
Hall, C.A., Chilcott, R.P., 2018. Eyeing up the future of the pupillary light reflex in neurodiagnostics. Diagnostics 8.
Heilman, K.M., Van Den Abell, T., 1980. Right hemisphere dominance for attention: the mechanism underlying hemispheric asymmetries of inattention (neglect). Neurology 30.
Hess, W.R., Buergi, S., Bucher, V., 1946. Motorische Funktionen des Tektal – und Tegmentalgebietes (motor functions of tectal and tegmental areas). Mon. Psychiatr. Neurol. 112, 1–52.
Hong, L., Walz, J.M., Sajda, P., 2014. Your eyes give you away: prestimulus changes in pupil diameter correlate with poststimulus task-related EEG dynamics. PLOS One 9.
Hsu, T. -Y., Hsu, Y. -F., Wang, H. -Y., Wang, C.-A., 2021. Role of the frontal eye field in human pupil and saccade orienting responses. Eur. J. Neurosci. 15253. ⟨https://onlinelibrary.wiley.com/doi/10.1111/ejn.15253⟩.
Hsu, T.-Y., Wang, H.-Y., Chen, J.-T., Wang, C.-A., 2022. Investigating the role of human frontal eye field in the pupil light reflex modulation by saccade planning and working memory. Front. Hum. Neurosci. 0 (793). ⟨https://www.frontiersin.org/articles/10.3389/fnhum.2022.1044893/full⟩.
Hsu, Y.-F., Baird, T., Wang, C.-A., 2020. Investigating cognitive load modulation of distractor processing using pupillary luminance responses in the anti-saccade paradigm. Eur. J. Neurosci. 52, 3061–3073 (Available at). ⟨https://onlinelibrary.wiley.com/doi/abs/10.1111/ejn.14736⟩.
Huang, Y.Z., Edwards, M.J., Rounis, E., Bhatia, K.P., Rothwell, J.C., 2005. Theta burst stimulation of the human motor cortex. Neuron.
Huerta, M.F., Krubitzer, L.A., Kaas, J.H., 1986. Frontal eye field as defined by intracortical microstimulation in squirrel monkeys, owl monkeys, and macaque monkeys: I. Subcortical connections. J. Comp. Neurol. 253.
James G., Witten D., Hastie T., Tibshirani R. , 2013 An Introduction to Statistical Learning, Springer Texts.
Johnston K., Everling S. , 2011. Frontal cortex and flexible control of saccades. Oxford Handb eye movements:279–302.
Joshi, S., Gold, J.I., 2020. Pupil size as a window on neural substrates of cognition. Trends Cogn. Sci. 24, 466–480.
Joshi, S., Li, Y., Kalwani, R.M., Gold, J.I., 2016. Relationships between pupil diameter and neuronal activity in the locus coeruleus, colliculi, and cingulate cortex. Neuron 89, 221–234 (Available at). ⟨http://linkinghub.elsevier.com/retrieve/pii/S089662731501034X⟩.
Karatekin, C., Bingham, C., White, T., 2010. Oculomotor and pupillometric indices of pro- and antisaccade performance in youth-onset psychosis and attention deficit/hyperactivity disorder. Schizophr. Bull. 36, 1167–1186.
Kardon, R., 1995. Pupillary light reflex. Curr. Opin. Ophthalmol. 6, 20–26.
Kawasaki, A., Ouanes, S., Crippa, S.V., Popp, J., 2020. Early-stage Alzheimer's disease does not alter pupil responses to colored light stimuli. J. Alzheimer's Dis. 75.
Komatsu, H., Suzuki, H., 1985. Projections from the functional subdivisions of the frontal eye field to the superior colliculus in the monkey. Brain Res. 327, 324–327.
Krauzlis, R.J., Lovejoy, L.P., Zenon, A., 2013. Superior colliculus and visual spatial attention. Annu Rev. Neurosci. 36, 165–182.
Künzle, H., Akert, K., 1977. Efferent connections of cortical, area 8 (frontal eye field) in Macaca fascicularis. a reinvestigation using the autoradiographic technique. J. Comp. Neurol. 173.

Laughlin, S.B., 1992. Retinal information capacity and the function of the pupil. Ophthalmic Physiol. Opt. 12, 161–164 (Available at). ⟨http://doi.wiley.com/10.1111/j.1475-1313.1992.tb00281.x⟩.
Lehmann, S.J., Corneil, B.D., 2016. Transient pupil dilation after subsaccadic microstimulation of primate frontal eye fields. J. Neurosci. 36, 3765–3776 (Available at). ⟨http://www.ncbi.nlm.nih.gov/pubmed/27030761⟩.
Leichnetz, G.R., 1982. Connections between the frontal eye field and pretectum in the monkey: an anterograde/retrograde study using HRP GEL and TMB neurohistochemistry. J. Comp. Neurol. 207.
Loewenfeld, I.E., 1999. The Pupil: Anatomy, Physiology, and Clinical Applications. Butterworth- Heinemann,, Boston.
Mathôt, S., Van der Stigchel, S., 2015. New light on the mind's eye: the pupillary light response as active vision. Curr. Dir. Psychol. Sci. 24, 374–378. ⟨http://www.ncbi.nlm.nih.gov/pubmed/26494950⟩.
Mathôt, S., Fabius, J., Van Heusden, E., Van der Stigchel, S., 2018. Safe and sensible preprocessing and baseline correction of pupil-size data. Behav. Res. Methods 50, 94–106. https://doi.org/10.3758/s13428-017-1007-2.
May, P.J., 2006. The mammalian superior colliculus: laminar structure and connections. Prog. Brain Res. 151, 321–378 (Available at). ⟨http://www.ncbi.nlm.nih.gov/pubmed/16221594⟩.
May, P.J., Warren, S., Bohlen, M.O., Barnerssoi, M., Horn, A.K.E., 2016. A central mesencephalic reticular formation projection to the Edinger-Westphal nuclei. Brain Struct. Funct. 221, 4073–4089 (Available at). ⟨http://www.ncbi.nlm.nih.gov/pubmed/26615603⟩.
May, P.J., Reiner, A., Gamlin, P.D., May, P.J., Reiner, A., Gamlin, P.D., 2019. Autonomic regulation of the eye. Oxf. Res. Encycl. Neurosci. 1–27.
McDougal, D.H., Gamlin, P.D., 2015. Autonomic control of the eye. Compr. Physiol. 5, 439–473 (Available at). ⟨http://doi.wiley.com/10.1002/cphy.c140014⟩.
Moschovakis, A.K., Karabelas, A.B., Highstein, S.M., 1988. Structure-function relationships in the primate superior colliculus. II. Morphological identity of presaccadic neurons. J. Neurophysiol. 60, 263–302.
Muggleton, N.G., Juan, C.H., Cowey, A., Walsh, V., 2003. Human frontal eye fields and visual search. J. Neurophysiol. 89, 3340–3343. Available at: www.jn.org [Accessed February 2, 2021].
Murphy K.P. , 2012. Machine learning: a probabilistic perspective (adaptive computation and machine learning series).
Nassar, M.R., Rumsey, K.M., Wilson, R.C., Parikh, K., Heasly, B., Gold, J.I., 2012. Rational regulation of learning dynamics by pupil-linked arousal systems. Nat. Neurosci. 15, 1040–1046. ⟨http://www.nature.com/doifinder/10.1038/nn.3130⟩.
Nyffeler, T., Wurtz, P., Lüscher, H.-R., Hess, C.W., Senn, W., Pflugshaupt, T., von Wartburg, R., Lüthi, M., Müri, R.M., 2006a. Extending lifetime of plastic changes in the human brain. Eur. J. Neurosci. 24, 2961–2966. ⟨http://doi.wiley.com/10.1111/j.1460-9568.2006.05154.x⟩.
Nyffeler, T., Wurtz, P., Lüscher, H.R., Hess, C.W., Senn, W., Pflugshaupt, T., von Wartburg, R., Lüthi, M., Müri, R.M., 2006b. Repetitive TMS over the human oculomotor cortex: comparison of 1-Hz and theta burst stimulation. Neurosci. Lett. 409, 57–60.
Nyffeler, T., Wurtz, P., Pflugshaupt, T., Wartburg, R., von, Luthi, M., Hess, C.W., Muri, R. M., 2006c. One-Hertz transcranial magnetic stimulation over the frontal eye field induces lasting inhibition of saccade triggering. Neuroreport 17, 273–275 (Available at). ⟨http://journals.lww.com/00001756-200602270-00009⟩.
Oh, A.J., Amore, G., Sultan, W., Asanad, S., Park, J.C., Romagnoli, M., Morgia, C.La, Karanjia, R., Harrington, M.G., Sadun, A.A., 2019. Pupillometry evaluation of melanopsin retinal ganglion cell function and sleep-wake activity in pre-symptomatic Alzheimer's disease. PLOS One 14.
Oster, J., Huang, J., White, B.J., Radach·, Ralph, Itti·, Laurent, Douglas·, Munoz, P., Wang·, Chin-An, 2022. Pupillary responses to differences in luminance, color and set size. Exp. Brain Res. 1, 1–13 (Available at). ⟨https://link.springer.com/article/10.1007/s00221-022-06367-x⟩.
Pinheiro, J.C., Bates, D.M., 2000. Mixed-Effects Models in S and S-PLUS (Statistics and Computing). Springer, NY.
Pong, M., Fuchs, A.F., 2000. Characteristics of the pupillary light reflex in the macaque monkey: Discharge patterns of pretectal neurons. J. Neurophysiol. 84, 964–974. ⟨https://pubmed.ncbi.nlm.nih.gov/10938320/⟩.
Prettyman, R., Bitsios, P., Szabadi, E., 1997. Altered pupillary size and darkness and light reflexes in Alzheimer's disease. J. Neurol. Neurosurg. Psychiatry 62, 665–668.
Raftery, A.E., 1995. Bayesian model selection in social research. Socio Method. 25.
Rodgers, C.K., Munoz, D.P., Scott, S.H., Pare, M., Paré, M., 2006. Discharge properties of monkey tectoreticular neurons. J. Neurophysiol. 95, 3502–3511 (Available at). ⟨http://www.ncbi.nlm.nih.gov/pubmed/16641382⟩.
Rossi, S., et al., 2009. Safety, ethical considerations, and application guidelines for the use of transcranial magnetic stimulation in clinical practice and research. Clin. Neurophysiol. 120, 2008–2039.
Rstudio Team , 2019. RStudio: Integrated development for R. RStudio, Inc., Boston MA. RStudio.
Sack, A.T., 2006. Transcranial magnetic stimulation, causal structure-function mapping and networks of functional relevance. Curr. Opin. Neurobiol. 16.
Sack, A.T., Kadosh, R.C., Schuhmann, T., Moerel, M., Walsh, V., Goebel, R., 2009. Optimizing functional accuracy of TMS in cognitive studies: a comparison of methods. J. Cogn. Neurosci. 21.
Schlag-Rey, M., Schlag, J., Dassonville, P., 1992. How the frontal eye field can impose a saccade goal on superior colliculus neurons. J. Neurophysiol. 67, 1003–1005 (Available at). ⟨https://journals.physiology.org/doi/abs/10.1152/jn.1992.67.4.1003⟩.
Scudder, C.A., Moschovakis, A.K., Karabelas, A.B., Highstein, S.M., 1996. Anatomy and physiology of saccadic long-lead burst neurons recorded in the alert squirrel monkey. I. Descending projections from the mesencephalon. J. Neurophysiol. 76, 332–352 (Available at). ⟨http://www.ncbi.nlm.nih.gov/pubmed/8836229⟩.
Scudder, C.A., Kaneko, C.R., Fuchs, A.F., 2002. The brainstem burst generator for saccadic eye movements: a modern synthesis. Exp. Brain Res. 142, 439–462.
Segraves, M.A., Goldberg, M.E., 1987. Functional properties of corticotectal neurons in the monkey's frontal eye field. J. Neurophysiol. 58, 1387–1419 (Available at). ⟨https://journals.physiology.org/doi/abs/10.1152/jn.1987.58.6.1387⟩.
Sokolov, E.N., 1963. Higher nervous functions: the orienting reflex. Annu. Rev. Physiol. 25, 545–580 (Available at). ⟨http://www.ncbi.nlm.nih.gov/pubmed/13977960⟩.
Sommer, M.A., Wurtz, R.H., 2000. Composition and topographic organization of signals sent from the frontal eye field to the superior colliculus. J. Neurophysiol. 83, 1979–2001.
Sommer, M.A., Wurtz, R.H., 2001. Frontal eye field sends delay activity related to movement, memory, and vision to the superior colliculus. J. Neurophysiol. 85, 1673–1685 (Available at). ⟨https://www.physiology.org/doi/10.1152/jn.2001.85.4.1673⟩.
Stanton, G.B., Goldberg, M.E., Bruce, C.J., 1988. Frontal eye field efferents in the macaque monkey: II. Topography of terminal fields in midbrain and pons. J. Comp. Neurol. 271, 493–506 (Available at). ⟨http://doi.wiley.com/10.1002/cne.902710403⟩.
Steinhauer, S.R., Hakerem, G., 1992. The pupillary response in cognitive psychophysiology and schizophrenia. Ann. N. Y Acad. Sci. 658, 182–204 (Available at). ⟨http://www.ncbi.nlm.nih.gov/pubmed/1497258⟩.
Thompson, K.G., Bichot, N.P., 2005. A visual salience map in the primate frontal eye field. Prog. Brain Res. 147, 249–262 (Available at). ⟨http://www.ncbi.nlm.nih.gov/pubmed/15581711⟩.
Van Stavern, G.P., Bei, L., Shui, Y.B., Huecker, J., Gordon, M., 2019. Pupillary light reaction in preclinical Alzheimer's disease subjects compared with normal ageing controls. Br. J. Ophthalmol. 103.
Wang, C.-A., Munoz, D.P., 2015. A circuit for pupil orienting responses: implications for cognitive modulation of pupil size. Curr. Opin. Neurobiol. 33, 134–140.
Wang, C.-A., Munoz, D.P., 2018. Neural basis of location-specific pupil luminance modulation. Proc. Natl. Acad. Sci. USA, 201809668 (Available at). ⟨http://www.pnas.org/lookup/doi/10.1073/pnas.1809668115⟩.
Wang, C.-A., Munoz, D.P., 2021. Coordination of pupil and saccade responses by the superior colliculus. J. Cogn. Neurosci. 33, 919–932. https://doi.org/10.1101/2020.08.20.247668.
Wang, C.-A., Munoz, D.P., 2023. Linking the superior colliculus to pupil modulation. In: Papesh, M., Goldinger, S. (Eds.), Modern Pupillometry: Cognition, Neuroscience, and Practical Applications. Springer.
Wang, C.-A., Boehnke, S.E., White, B.J., Munoz, D.P., 2012. Microstimulation of the monkey superior colliculus induces pupil dilation without evoking saccades. J. Neurosci. 32, 3629–3636.
Wang, C.-A., Brien, D.C., Munoz, D.P., 2015. Pupil size reveals preparatory processes in the generation of pro-saccades and anti-saccades. Eur. J. Neurosci. 41, 1102–1110.
Wang, C.-A., Huang, J., Yep, R., Munoz, D.P., 2018. Comparing pupil light response modulation between saccade planning and working memory. J. Cogn. 1 (33). ⟨https://www.journalofcognition.org/article/10.5334/joc.33/⟩.
White, B.J., Munoz, D.P., 2011. The superior colliculus. In: Liversedge Gilchrist, I., Everling, S.S. (Eds.), Oxford Handbook of Eye Movements. Oxford University Press, pp. 195–213.
Woodhouse, J.M., 1975. The effect of pupil size on grating detection at various contrast levels. Vis. Res 15, 645–648.
World Medical Association, 2001. World Medical Association Declaration of Helsinki. Ethical principles for medical research involving human subjects. Bull. World Health Organ 79, 373–374 (Available at). ⟨http://www.ncbi.nlm.nih.gov/pubmed/11357217⟩.
Yu, M., Kautz, M.A., Thomas, M.L., Johnson, D., Hotchkiss, E.R., Russo, M.B., 2007. Operational implications of varying ambient light levels and time-of-day effects on saccadic velocity and pupillary light reflex. Ophthalmic Physiol. Opt. 27.